Indian Institute of Technology, Kanpur

Project Report on finding

Effective engineering properties of Composite Material Using Different Micromechanics methods

Submitted to

Course Instructor: Dr. PM mohite

Course: (AE681A) Composite Materials

Submitted by

Name: Karan Kumar Tiwari

Dept: Aerospace Structure

Roll no: 22101028

Index:

1. Introduction:

Effective engineering properties of composite materials play a vital role in their design and analysis for various engineering applications. The effective properties are determined by the microstructure and the constituent materials of the composite. Several micromechanics methods have been developed to predict the effective properties of composite materials. In this project report, we focus on evaluating different micromechanics methods for finding the effective engineering properties of composite materials. Specifically, we will investigate the effectiveness of methods such as the Mori-Tanaka, Halpin-Tsai, and Voigt-Reuss models, Concentric cylinder approach and others, for determining the effective stiffness, strength, and Poisson's ratios of composite materials. By comparing and analyzing the results obtained from these methods, we hope to provide insights into the advantages and limitations of different micromechanics models for composite analysis and to develop a better understanding of the factors influencing the effective engineering properties of composite materials. The outcomes of this study can be useful in developing new and improved composite materials for various engineering applications.

2.Material and properties:

Given $V_f = 0.6$

Fiber**:** Silenka E-glass 1200tex

Fibre properties	
Longitudinal modulus, E1 (GPa)	74
Transverse modulus, E2 (Gpa)	74
In-plane shear modulus, G12 (GPa)	30.8
Major Poisson’s ratio, v12	0.2
Transverse shear modulus, G23(GPa)	30.8

Matrix **:** LY556/HT907/DY063

Modulus, Em (GPa)	3.35
Poisson’s ratio, νm	0.35

3.1 Strength of Material approach:

- four out of five engineering constants are obtained in this method
- E_1*, E_2*=E_3*, Nu12=Nu13 G_{12}*=G_{13}*
- E2* without deformation follows rule of mixture

$$\frac{1}{E_2^*} = \frac{V_f}{E_2^{(f)}} + \frac{V_m}{E^{(m)}}$$

- whereas E2* with consideration of deformation in axial direction also follows rule of mixture with non-dimensional term $\eta^{(f)}$ and $\eta^{(m)}$

$$\frac{1}{E_2^*} = \frac{\eta^{(f)} V_f}{E_2^{(f)}} + \frac{\eta^{(m)} V_m}{E^{(m)}}$$

- Hence, we can see the effect of scaled value of E2* due to non dim. term as in E2* with deformation plot.

3.2 Hill's concentration method and standard mechanic's approach:

In this method we are using Abaqus CAE software for RVE analysis, RVE has two phases as fiber and matrix and their effective properties are as follow.

Length of RVE	15mm
Height of RVE	15mm
Width of RVE	15mm
Volume of fiber in RVE	2.01773E+03
Volume of matrix in RVE	1.35727E+03
Number of nodes in Mesh	5024
Total number of elements	4275
Load Applied on RVE in normal directions	0.01 Mpa
Shear loads	0.01 Mpa
Elements type	linear C3D8R hexahedral

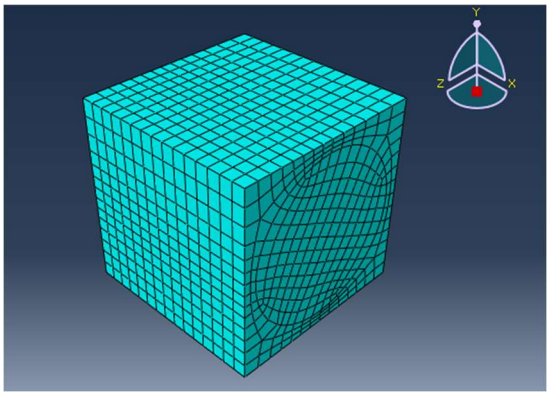

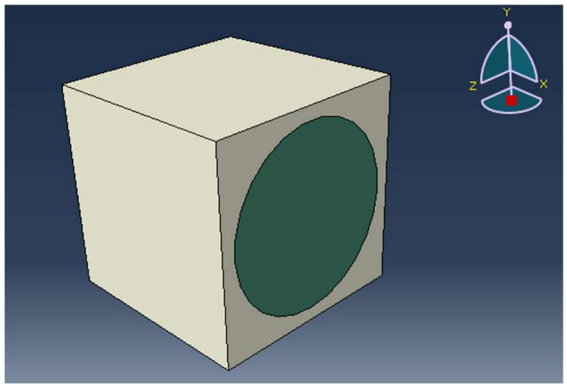

- In case of Homogeneous traction boundary condition, we will get average values of stresses for every elemental volume

  Traction, $T_i = \sigma_{ij} n_j$,

  with σ_{ij} is a constant state of stress,

  then the average stress in composite is σ_{ij}
- Now we do ananlysis of our RVE for 3 normal and 3 shear stress conditions

For $\boldsymbol{\sigma_{xx}}$

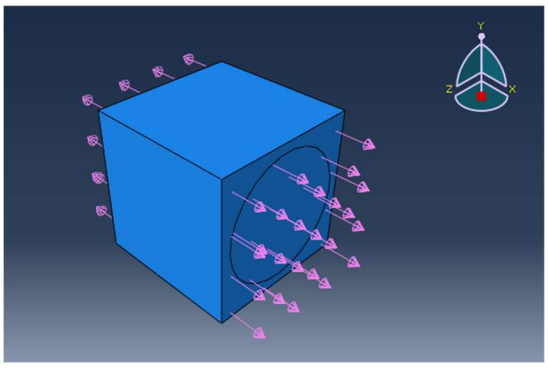

Load For $\boldsymbol{\sigma_{zz}}$

For $\boldsymbol{\sigma_{yy}}$

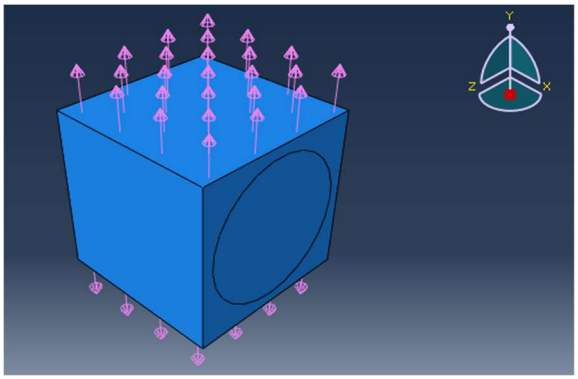

Load For $\boldsymbol{\sigma_{xy}}$

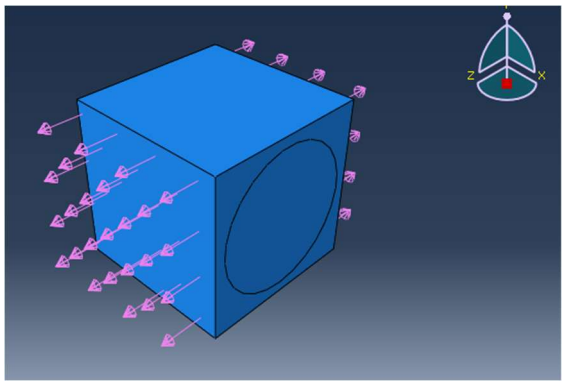

Load For $\boldsymbol{\sigma_{xz}}$

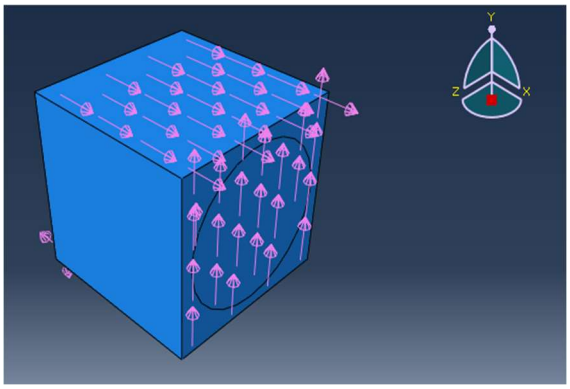

Load For $\boldsymbol{\sigma_{yz}}$

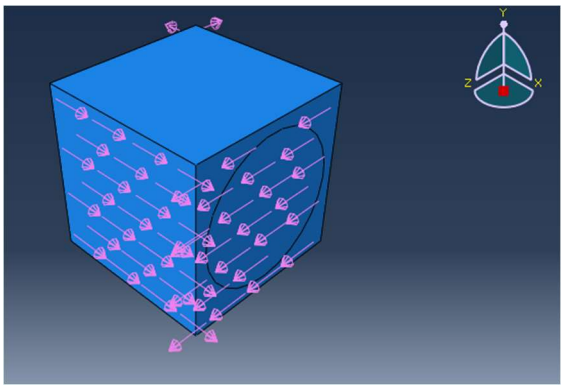

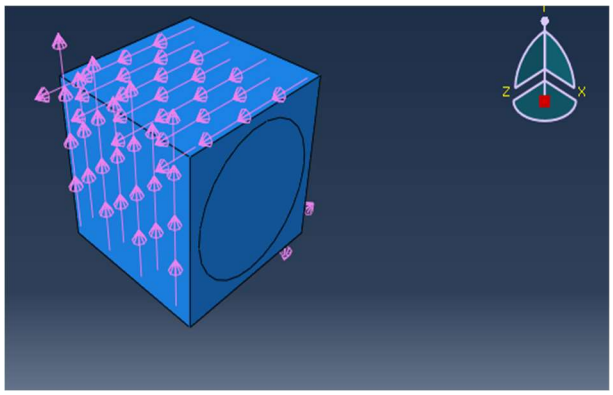

Resulting Stresses

A. For σ_{xx}

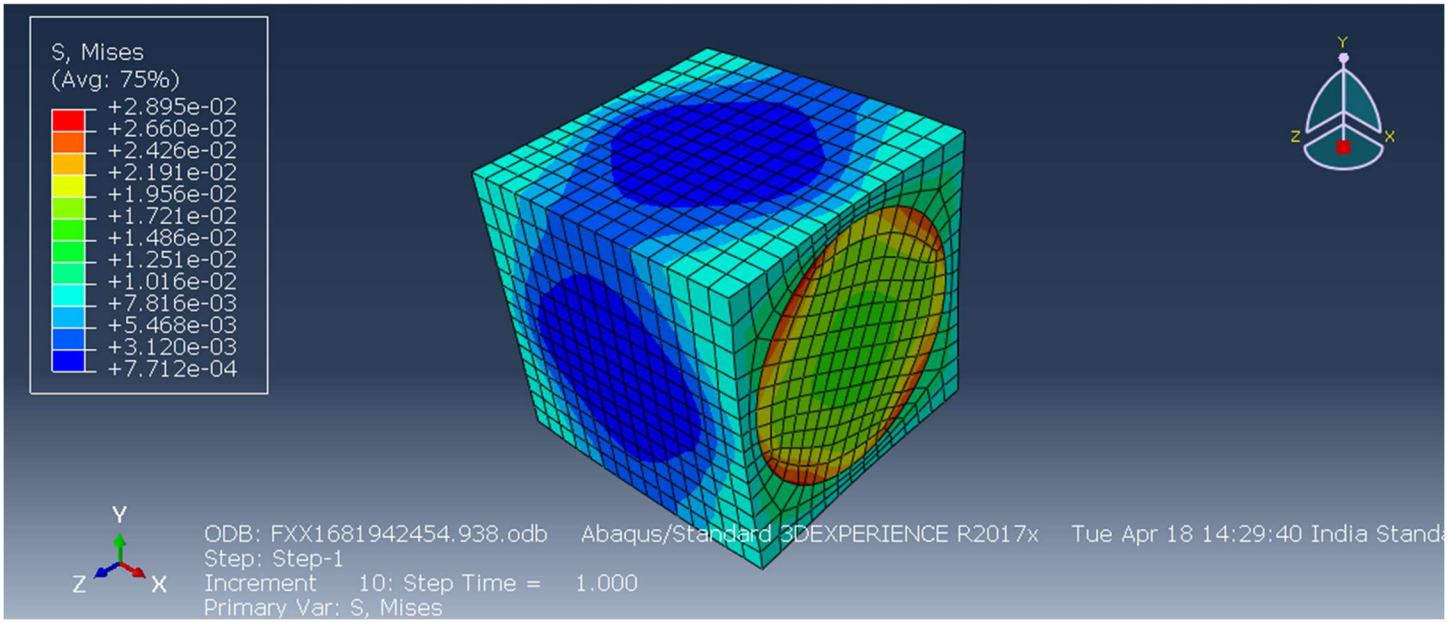

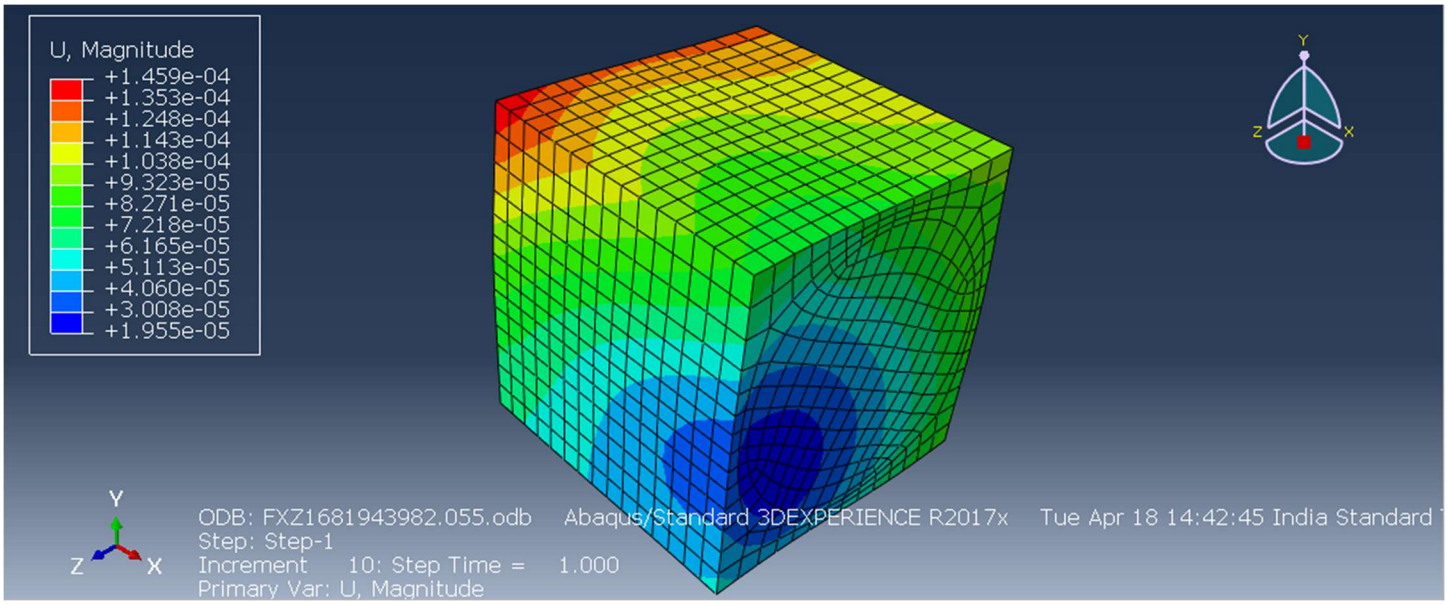

B.For σ_{yy}

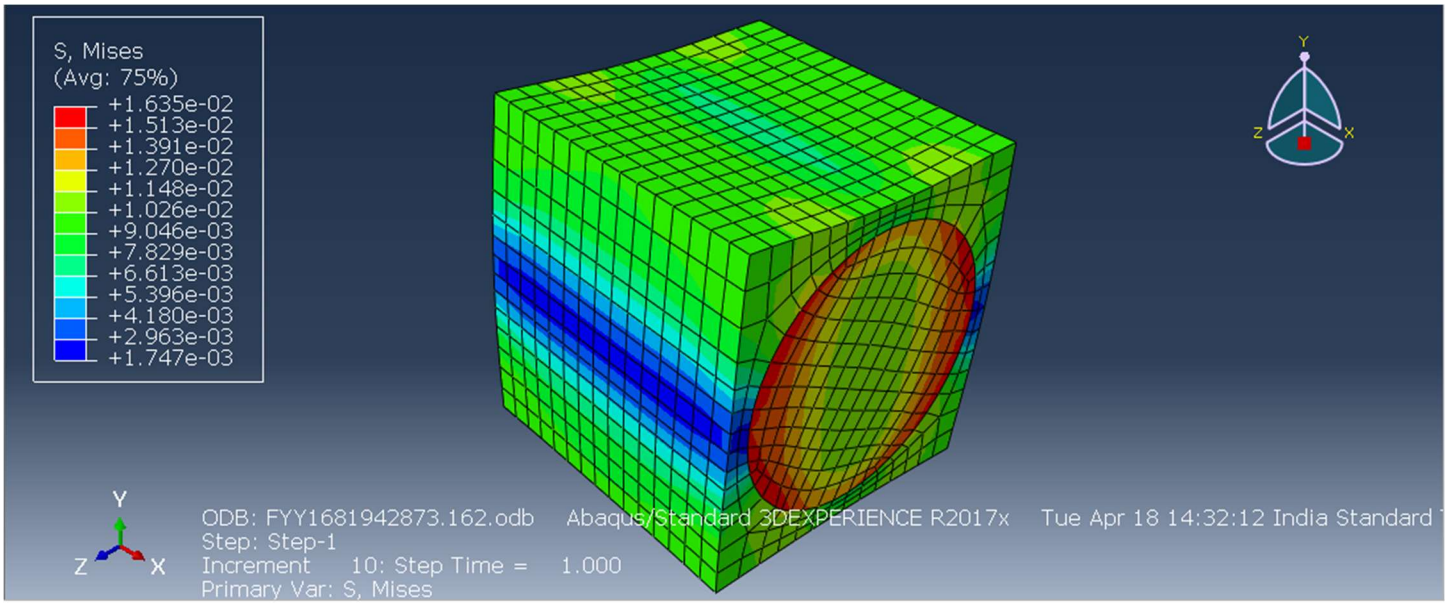

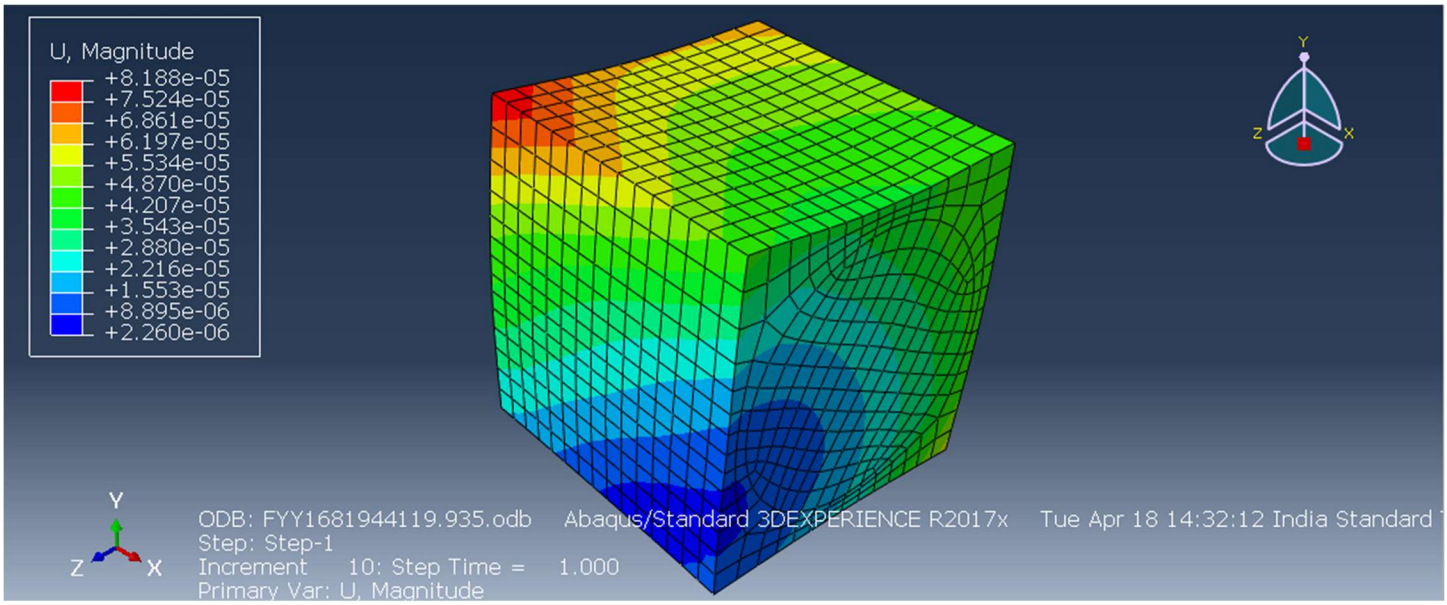
U, Magnitude
+8.188e-05
+7.524e-05
+6.861e-05
+6.197e-05
+5.534e-05
+4.870e-05
+4.207e-05
+3.543e-05
+2.880e-05
+2.216e-05
+1.553e-05
+8.895e-06
+2.260e-06
Y
Z
X
ODB: FYY1681944119.935.odb Abaqus/Standard 3DEXPERIENCE R2017x Tue Apr 18 14:32:12 India Standard
Step: Step-1
Increment 10: Step Time = 1.000
Primary Var: U, Magnitude

C.σ_{zz}

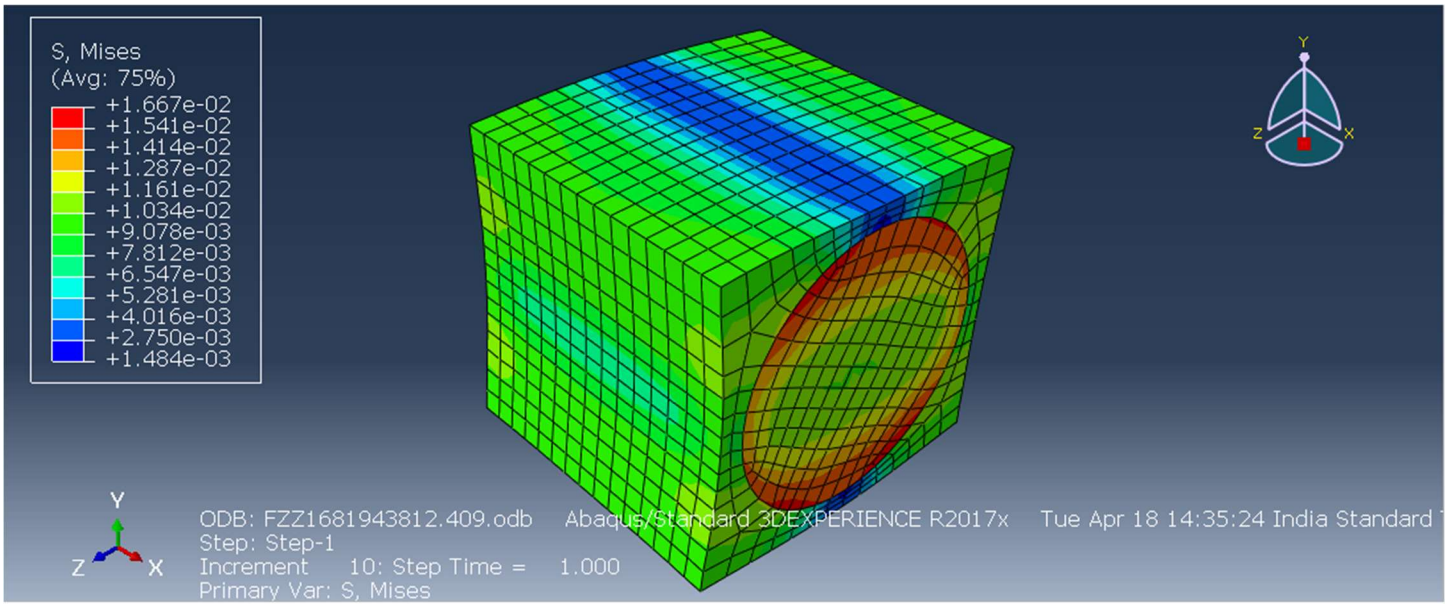
S, Mises
(Avg: 75%)
+1.667e-02
+1.541e-02
+1.414e-02
+1.287e-02
+1.161e-02
+1.034e-02
+9.078e-03
+7.812e-03
+6.547e-03
+5.281e-03
+4.016e-03
+2.750e-03
+1.484e-03
Y
Z
X
ODB: FZZ1681943812.409.odb Abaqus/Standard 3DEXPERIENCE R2017x Tue Apr 18 14:35:24 India Standard
Step: Step-1
Increment 10: Step Time = 1.000
Primary Var: S, Mises

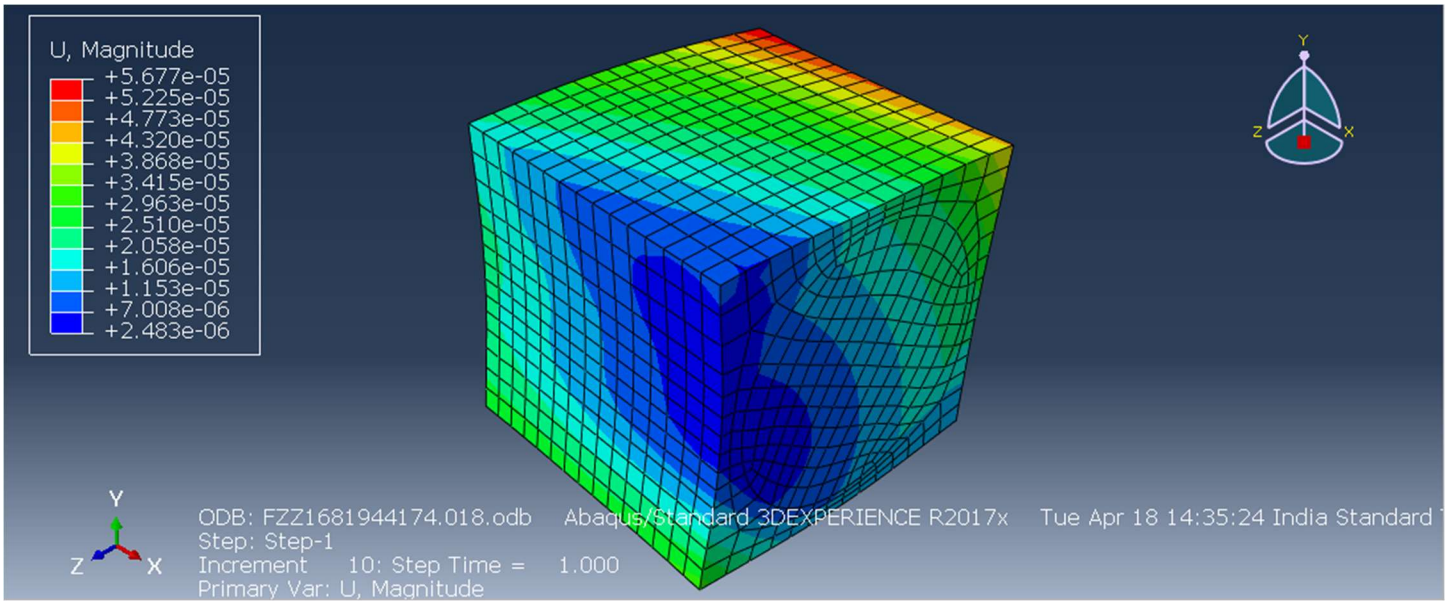

D. For σ_{xy}

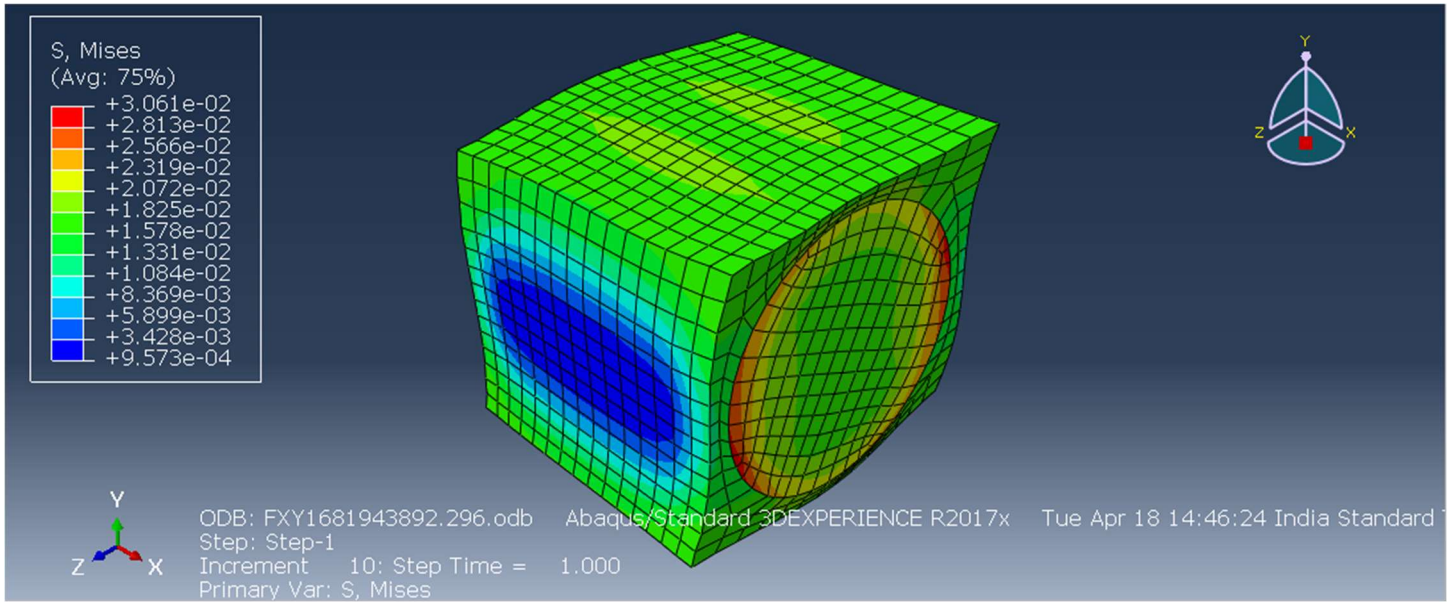

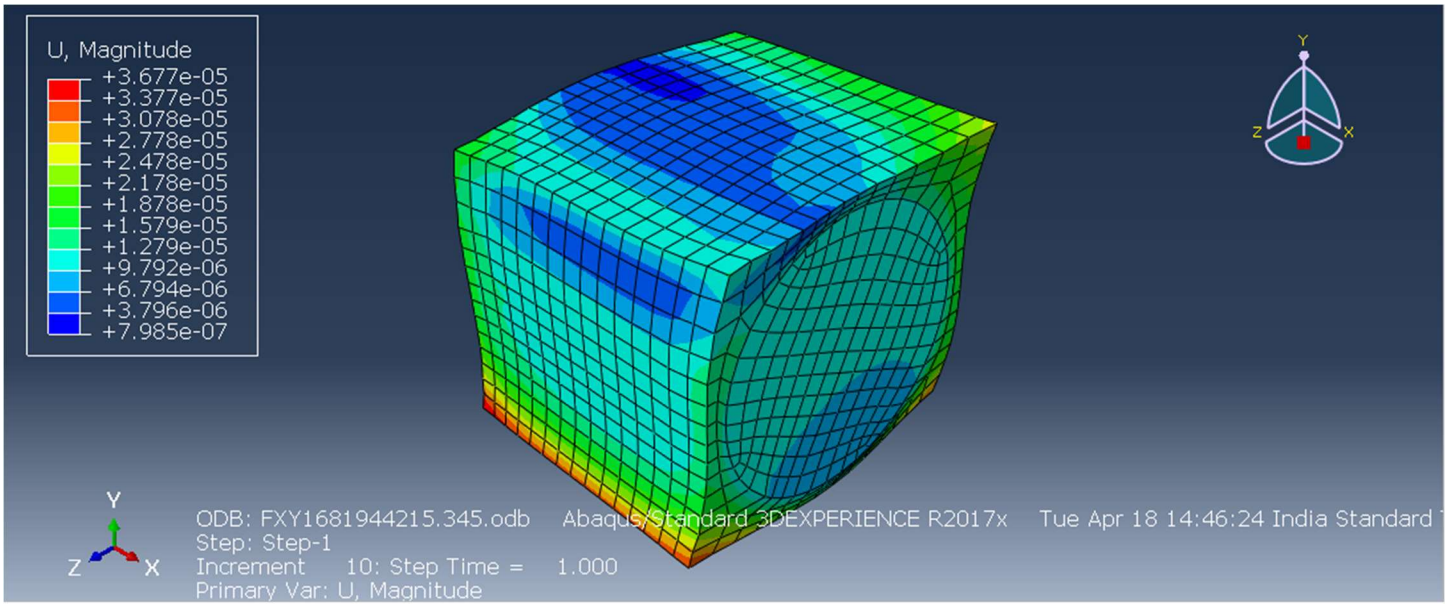

E. For σ_{xz}

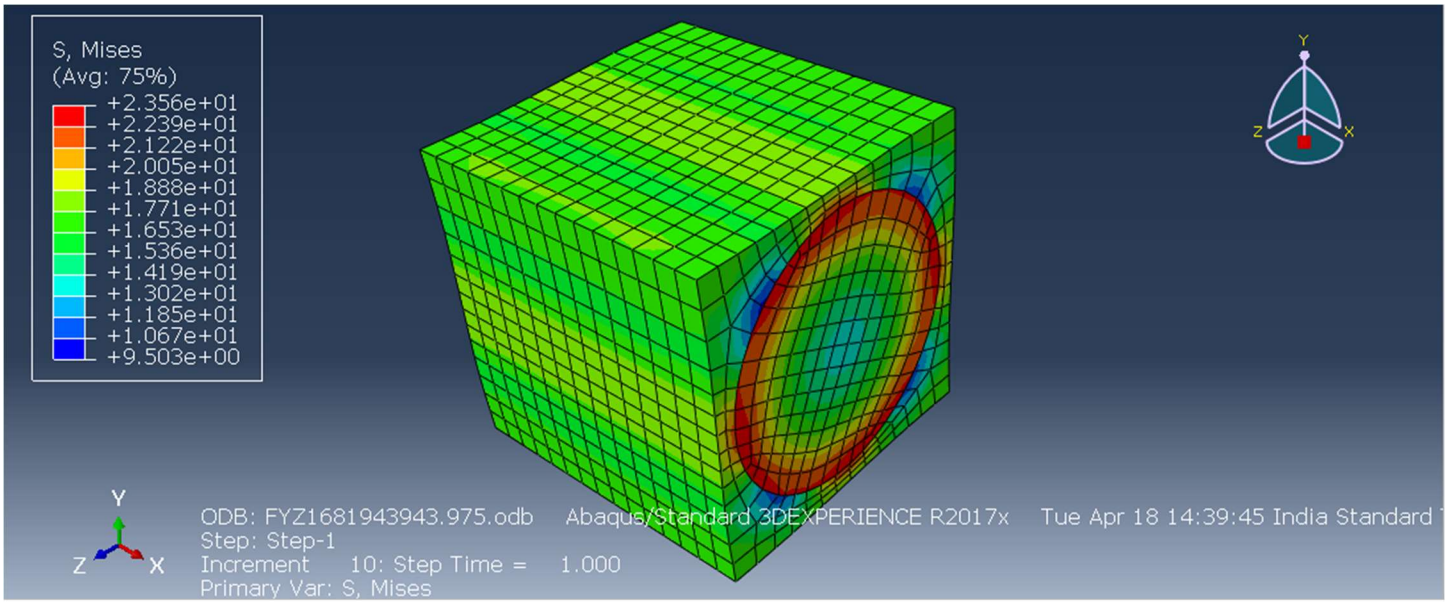

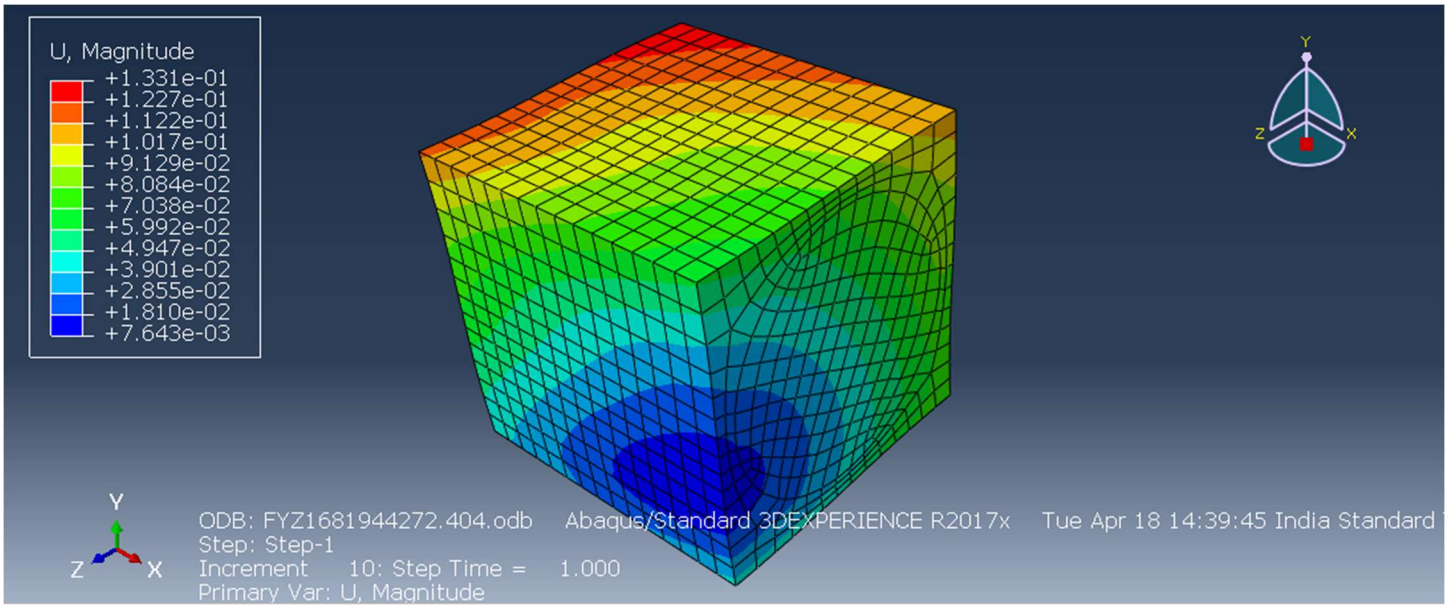

F. For σ_{yz}

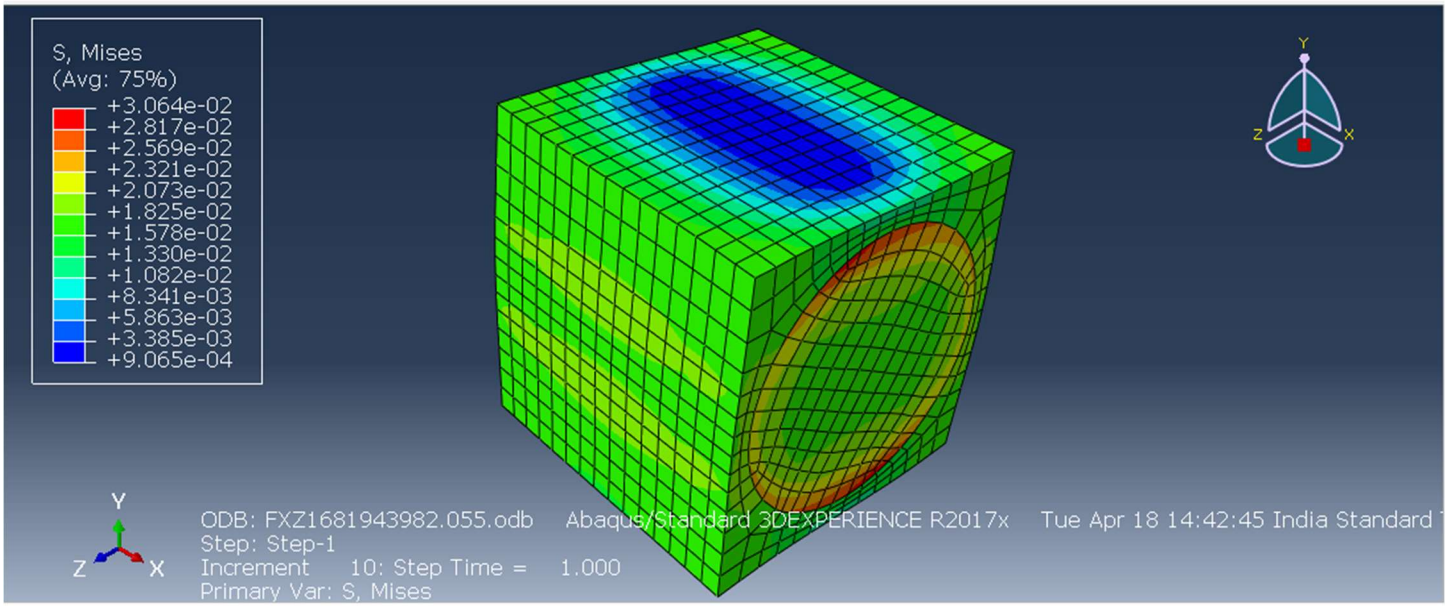

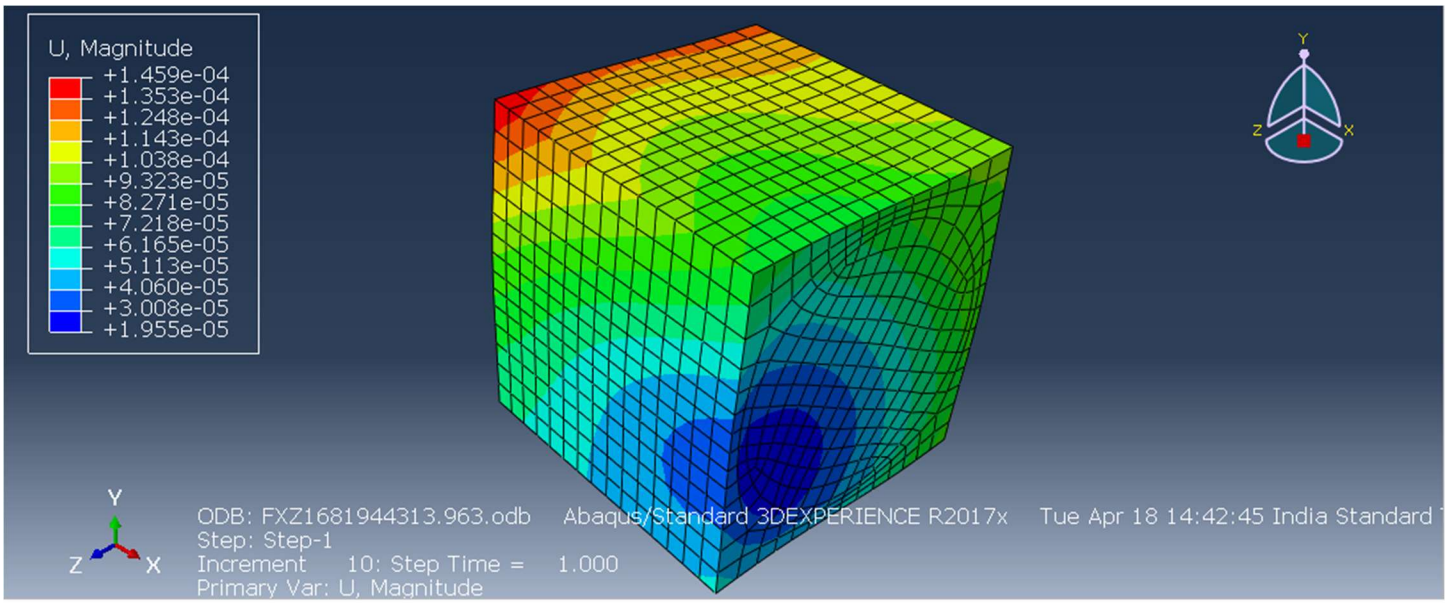

- With the help of Hill's analysis fibre and matrix phase averaged concentration factor is calculated

$$\mathbf{V_f * B^{(f)}_{ijkl} + V_m * B^{(m)}_{ijkl} = I_{ijkl}}$$

Where,

$B^{(m)}_{ijkl}$ - Stress concentration factor for matrix

$B^{(f)}_{ijkl}$ -Stress concentration factor for fiber

This equality must hold as it checks the analysis of engineering constants is satisfactory.

Final check matrix

	1	2	3	4	5	6
1	1.0021	0	0	0	0	0
2	0	1.0004	0	0	0	0
3	0	0	1.0004	0	0	0
4	0	0	0	1.0004	0	0
5	0	0	0	0	1.0009	0
6	0	0	0	0	0	1.0009
7						

- Effective Properties from RVE analysis using hills approach

Axial modulus E^*_1	16.7287Gpa
Transverse axial modulus E^*_2	92.488 Gpa
In plane shear modulus G^*_{12}	3.82322 Gpa
Transverse shear modulus G^*_{23}	3.2103 Gpa
In plane Poisson's ratio ν^*_{12}	0.29

3.3 Voigt Approximation:

- Voigt assumed that the strains are constants throughout the composite.
- It Gives Upper bound for C^*_{11} ,$C^*_{22,}$ C^*_{44} ,C^*_{66} and lower bound for C^*_{12} ,$C^*_{13,}$ C^*_{23} of stiffness matrix.
- It Gives Upper bound for S^*_{12} ,$S^*_{13,}$ S^*_{23} and lower bound for S^*_{11} ,$S^*_{22,}$ S^*_{44} ,S^*_{66} of compliance matrix.

$$\mathbf{C^*_{ijkl} = V_f * C^{(f)}_{ijkl} + V_m * C^{(m)}_{ijkl}}$$

3.4 Reuss Approximation

- Reuss assumed that the stress are constants throughout the composite.
- It Gives lower bound for C^*_{11} ,$C^*_{22,}$ C^*_{44} ,C^*_{66} and Upper bound for C^*_{12} ,$C^*_{13,}$ C^*_{23} of stiffness matrix.

- It Gives Lower bound for S^*_{12} ,$S^*_{13,}$ S^*_{23} and Upper bound for S^*_{11} ,$S^*_{22,}$ S^*_{44} ,S^*_{66} of compliance matrix.

$$\mathbf{S^*_{ijkl} = V_f * S^{(f)}_{ijkl} + V_m * S^{(m)}_{ijkl}}$$

3.5 CCA Method:

- In this model a composite is represented as an assemblage of concentric cylinders.
- The core of this cylinder is a fiber and surrounding annulus is a matrix material.

Steps of CCA method:

- Define the geometry

  b=0.1 radius of outer annulus
  a=b*sqrt(V_f) radius of inner annulus

- Assignment of properties of each phase

- Calculation of effective properties of the composite using boundary and continuity condition and using appropriate mathematical relations.

- G_{23*} is calculated using three- phase cylinder model with appropriate boundary conditions.

3.6 Mori-Tanaka Method:

- Here, also composite material is represented as a two-phase system, with one phase being the "matrix" material and the other phase being the "inclusion" material**.**
- Using the boundary conditions of the model we calculate the strain field within the composite material.
- Then we solve for effective properties using Mori-Tanaka equations.

3.7 Halpin-Tsai Semi-Empirical Relations:

- Calculation of E_1* and ν^*_{12} is done using Rule of mixture.
- Then we calculate hills moduli using Halpin-Tsai semi-empirical relations.
- Then we calculate effective properties

3.8 Hashin–Shtrikman bounds:

- Provides upper and lower limits on the effective properties of the composite material.
- Variational principles involving the polarization tensor used.
- Principle of minimum potential energy and minimum complementary energy is used.

4. Observation and Prediction: Plots for all methods for E_1*, E_2*, G_{12*}, G_{23*}, ν^*_{12}, ν^*_{23}

Fig. 1

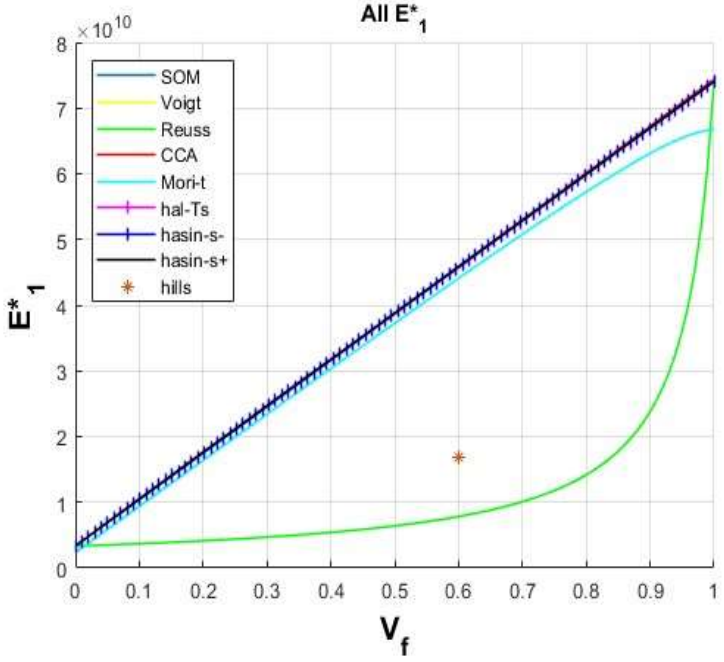

Fig. 2

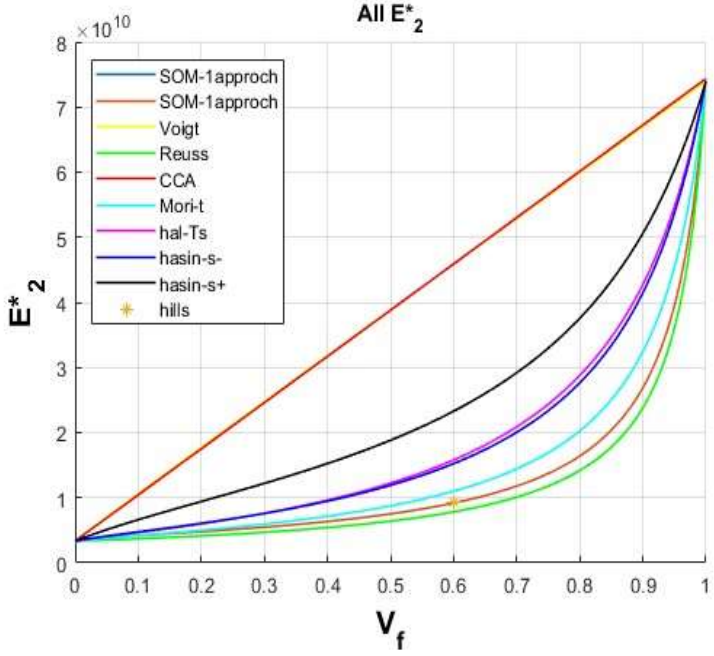

Fig. 3

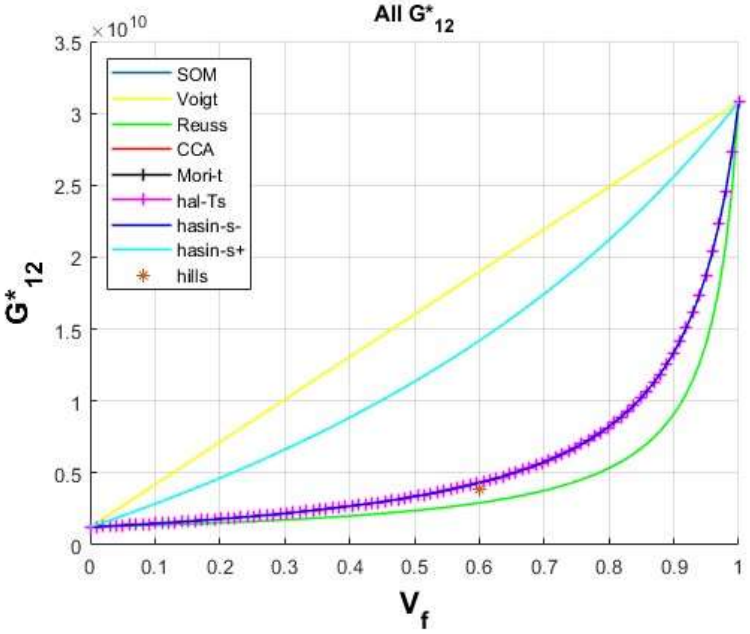

Fig. 4

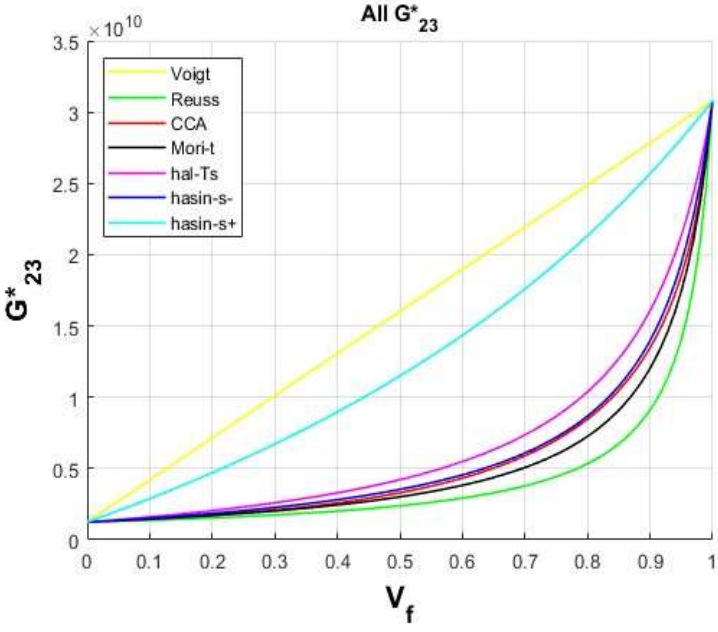

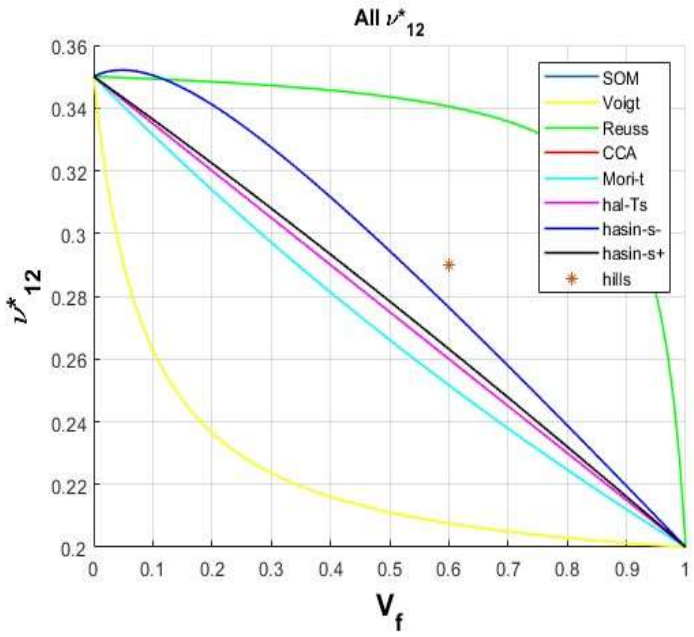

Fig. 5

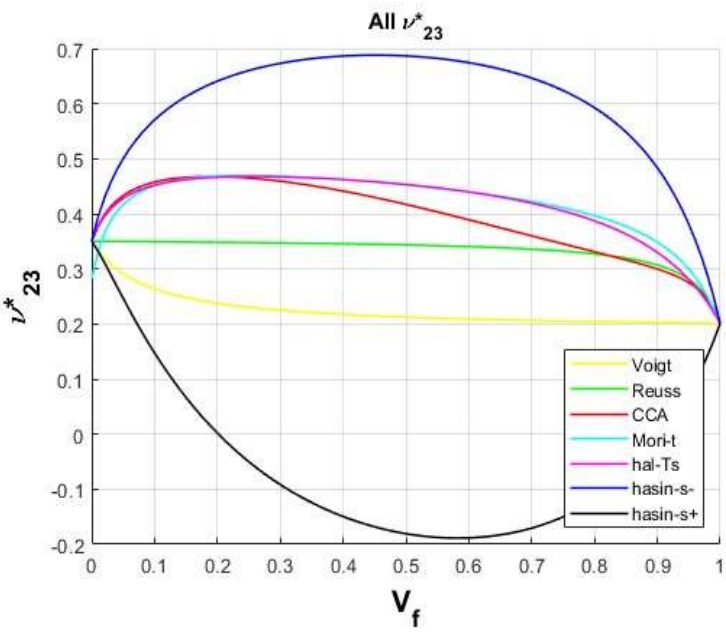

Fig. 6

Figure 1:

- Here all models other than Reuss predict the same results for effective properties predicts the same results for effective axial modulus E1*.
- Reuss model assumes that axial stresses are same in each phase of composite which is not true as fiber and matrix have different moduli are subjected to same uniform strain.

Figure 2:

- As fiber is stiffer than the matrix and contributes more to the stiffness of composite hence the effective transverse modulus generally increases with increasing volume fraction of the reinforcing phase.
- Here as we can see all models predict highly nonlinear behavior for Transverse modulus with the exception of Voigt model which assumes uniform strains throughout the composite.
- Here we can see Voigt and Reuss are giving upper and lower bound foe E_2 while some methods are predicting reasonably close result to each other.

Figure 3 and 4:

- Here Voigt and Reuss are giving upper and lower bound and excluding Hasin-Strikman positive bound all other methods are converging at the same curve.
- For Isotropic constituents of composite, the behavior of plots for E_2*,G_{12}*, G_{23}* are almost similar .

- Here the slope of the effective axial shear modulus vs. volume fraction curve is different for different methods.

Figure 5: In Plane Poisson ratio ν^*_{12}

- Here we see as the volume fraction of the reinforcing phase increases, the axial Poisson's ratio of the composite material typically decreases. This is because the fiber is stiffer than the matrix phase, which results in a lower overall Poisson's ratio for the composite.
- Haplin-Tsi is predicting non linear behavior where as with the exception of Voigt and Reuss method all other methods are predicting linear variation of Poisson's ratio.
- Here the slope of the effective axial shear modulus vs. volume fraction curve is different for different methods.

Figure 6: Out of plane Poisson ratio ν^*_{23}

- Hain-stickman bounds are giving upper and lower bound for the values of out of plane Poisson's ratio.
- Here also we get to see the effect of increasing stiffness due to increase in fiber content and hence we get decrease in the value of ν^*_{23}, but this decrement is less severe in comparison to $\nu^*_{12.}$